

TABLE I

$\bar{\gamma}$	$\left(\frac{\partial \epsilon}{\partial \theta}\right)_{\bar{\gamma}}$	
	250° C	350° C
0.435		- 0.65
0.440		
0.450	- 0.68	
0.480		
0.500	- 0.80	
0.600		
0.620		
0.630		- 0.70
0.640	- 0.82	
0.700	- 0.65	- 0.40
0.800		
0.920		- 0.50
1.000	- 0.70	
1.200	- 0.63	- 0.70
1.400	- 0.72	- 0.65
1.500		
1.600	- 0.67	- 0.63
1.700	- 0.82	
1.790		- 0.76
1.800	- 0.80	
1.880		
2.000		- 0.60

constant - $\alpha/\beta = - 0.7$. The resemblance of the experimentally determined values of α/β to that given by equation 3 indicates that the Kovacs-Nagy (K-N) equation is valid.

References

1. I. KOVACS and P. FELTHAM, *Phys. Stat. Sol.* **3** (1963) 2379.
2. I. KOVACS and E. NAGY, *ibid* **8** (1965) 795.
3. F. A. GAYDON, *J. Mech. Appl. Math.* **5** (1952) 29.
4. S. HOWE and C. ELBAUM, *Phil. Mag.* **6** (1961) 37.
5. P. FELTHAM, *ibid* **8** (1963) 989.
6. T. H. YOUSEF, Ph.D Thesis, Cairo University (1967).

D.C. Hall Current Measurements on Organic Crystals

Hall voltage measurements of mobility against temperature normally used in the studies of conduction processes in semiconductors have serious limitations for high resistivity materials, such as organic solids. It is often impossible to separate surface and bulk effects for crystals of bulk resistivities greater than $10^2 \Omega m$. Resistivities greater than $10^8 \Omega m$ present difficulties associated with input impedance and sensitivity requirements of the detection system. The Hall current measurement technique first described by Dobrovolskii and Gritsenko [1] can overcome these difficulties if single crystals of suitable dimensions can be prepared.

Hall current measurements on anthracene have been reported [2] previously and here the

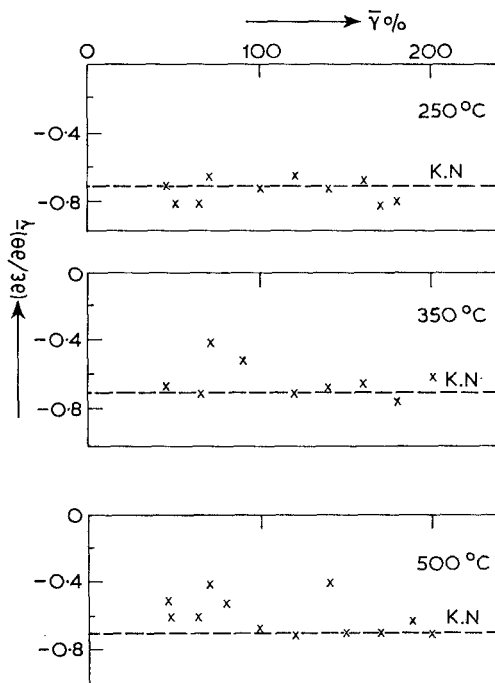


Figure 3 Variation of the relative change of tensile strain with plastic torsion $\partial \epsilon / \partial \theta$ vs. $\bar{\gamma}$.

Received 29 September

and accepted 12 October, 1970

M. R. SOLIMAN
G. A. HASSAN

National Research Centre, Cairo, UAR

F. H. HAMMAD

Department of Metallurgy, University of
Nottingham, UK

technique is detailed. The basic outline of the measuring circuit and the geometry of the specimen and electrodes are given in fig. 1. With this geometry the Hall field normally generated in the Hall voltage technique, is short circuited by the electrodes: one half of the resultant Hall current is detected across the split electrode $A_1 - A_2$. The surface effects are eliminated by the guard ring.

Measurements made in this laboratory on single crystal silicon specimens indicated that the accuracy of the Hall current technique depended critically on the contact resistances of the broad area electrodes. For silicon it was not possible to use the technique for material having resistivities over $1 \Omega m$, because satisfactory low resistance ohmic electrodes could not be fabricated with available equipment. The normal practice for conductivity measurements on

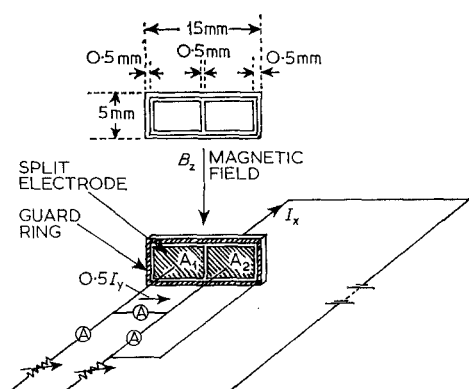


Figure 1 Electrode geometry and circuit for Hall current measurement.

organic crystals is to use simple pressure contacts or metallic paste coatings: this is permissible as the conduction parameters are usually greater than the noise generated in the contacts. However, for Hall measurements in organic crystals, the low charge carrier concentrations and mobilities result in Hall currents $< 10^{-15}$ A; in comparison the electrical noise of pressure or paste contacts is excessive and it is necessary to use vacuum deposited electrodes.

Each crystal of dimensions $15 \times 5 \times 1$ mm, with major faces cut either parallel or perpendicular to the ab cleavage plane, was held against the magnetic thermal sink by a steel mask machined to the pattern of fig. 2. The crystal surfaces were

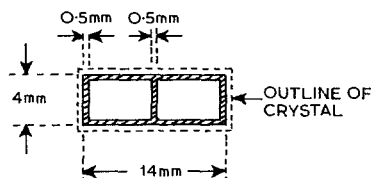


Figure 2 Electrode mask.

cleaned by allowing them to evaporate for a few minutes at a pressure of 10^{-4} torr. The crystals were cooled slowly to about 175° K before the gold was evaporated at 10^{-3} torr. The vacuum system was flushed with high purity argon before each pumping cycle and liquid nitrogen vessels froze out any water vapour. Light was excluded to avoid the production of photo-oxides.

Details of the measurement cell are shown in fig. 3. The cell was light tight and maintained a vacuum of better than 10^{-3} torr. Satisfactory thermal stability and insulation resulted from the use of massive sections of aluminium and the

demountable "Dewar" comprised of the aluminium and silvered glass jacket. The split electrode and guard ring contact assembly was fabricated by grinding and cutting a brass electrode which had been potted in epoxy resin under vacuum. The room temperature leakage resistance between each half of the split electrode and between this electrode and the guard ring was greater than $10^{14} \Omega$ under vacuum. Carbon dispersed polyethylene provided pliable contacts to the gold electrodes on the crystal surfaces and these were attached to the brass electrode segments using "dag" silver dispersion as an adhesive. The pliable contacts allowed for differential thermal expansion and for any slight errors in crystal cutting. The specimens and electrode assemblies were held in position by a phosphor bronze spring and a thermocouple junction was cemented into the fixed brass electrode assembly. Temperature control was achieved using heating tape and by passing liquid nitrogen through the aluminium base. The cell was positioned with the crystal specimen located centrally between the 4 ins. diameter poles of an electromagnet.

The circuit used to measure the Hall current is shown in fig. 4. R_1 and V_1 (Wayne Kerr M 141) were used to establish the guard ring and the split electrode at the same potential. R_2 and A_1 (Wayne Kerr M 141) were used to balance the measuring circuit. Electrometers A_2 and A_3 (Rank Cintel DC amplifiers NE 503B) measured the total crystal current. To satisfy earthing requirements, A_3 had to be disconnected during Hall current measurement. At room temperature, and below, R_3 , R_4 and R_5 were $10^{13} \Omega$ resistors. For higher temperatures the bridge sensitivity was optimised by using 10^{12} or $10^{11} \Omega$ resistors.

After the circuit had been in equilibrium for at least 2 h it was balanced, with the magnetic field applied, using A_1 . On reversing the magnetic field, A_1 indicated twice the Hall current short circuited by the split electrode. Further reversals of the field allowed readings to be averaged. The electrical noise was reduced by a 220 pF capacitor across the input of A_1 this increased the indication time to 15 min. For applied voltages greater than 700 V the stability was too low for measurements to be made.

The temperature range of measurement was limited to 275 to 360° K; below this both balancing the circuit and detecting the Hall current were difficult; above this it was impossible to maintain thermal equilibrium of the crystal for the measurement time.

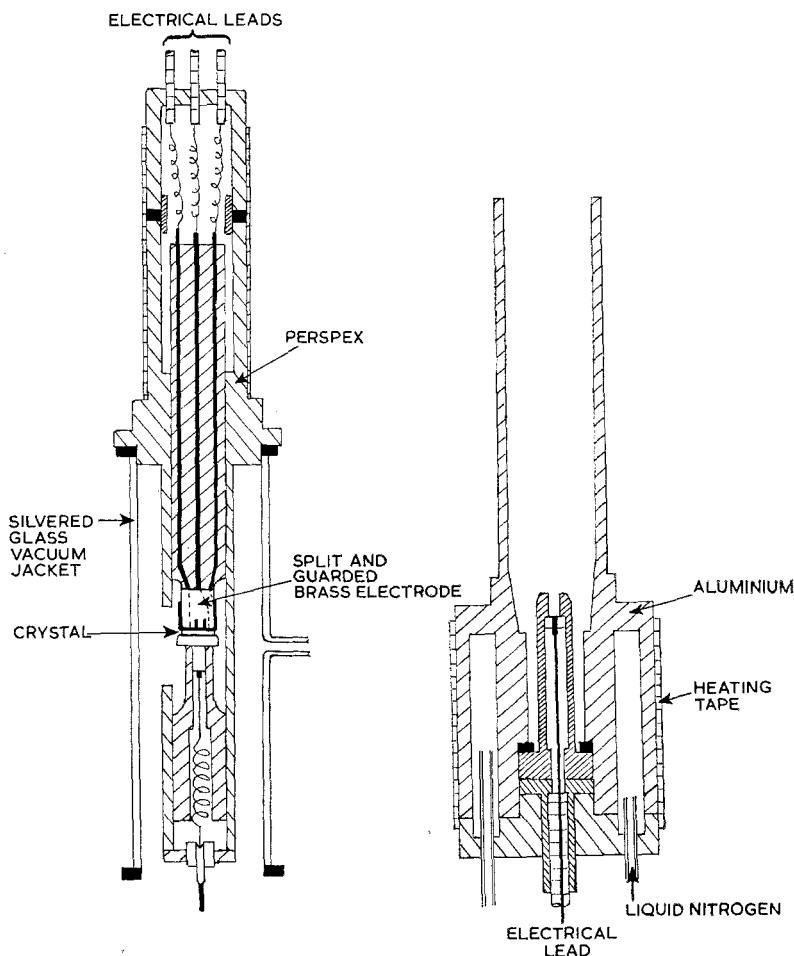


Figure 3 Hall current measurement cell.

Using the terminology of reference [1], a simple correction for the crystal resistivity anisotropy gives the Hall current as

$$I_y = -\frac{\rho_x}{\rho_y} \frac{a}{b} \mu_H B_z I_x$$

(in reference [2] this was mistakenly printed as ρ_y/ρ_x); typically at 298° K, 6×10^5 V/m and 0.71T the Hall currents were 1.0×10^{-15} A and 8.0×10^{-16} A, perpendicular and parallel to the cleavage plane of anthracene. The corresponding electron Hall mobilities were 1.3×10^{-4} and 5.0×10^{-4} m²/Vs. Subsequent mass spectroscopic and fluorescence measurements [3] indicated that the anthracene crystals contained about 50 ppm tetracene. Schmillen and Falter [4] obtained hole drift mobility values of the order 5×10^{-6} m²/Vs for 50 ppm tetracene doped

anthracene crystals. Using these values gives ratios of Hall mobility to drift mobility of 26 and 100, which are of the order of magnitude and anomalous sign predicted by Friedman [5] for the narrow band description of carrier transport in anthracene.

Schadt and Williams [6] report DC dark Hall current mobility values in anthracene at 293° K of the same order as those obtained in this laboratory, and find no anomalous behaviour in the *ab* plane consistent with a conduction mechanism described by a hopping, rather than a band model. Theoretical studies [7] of the drift mobility in anthracene indicate that the dominant transport mechanism depends on the crystallographic direction. It is considered that the physical state of the crystal (e.g. impurity content, defect structure etc.), and the experimental

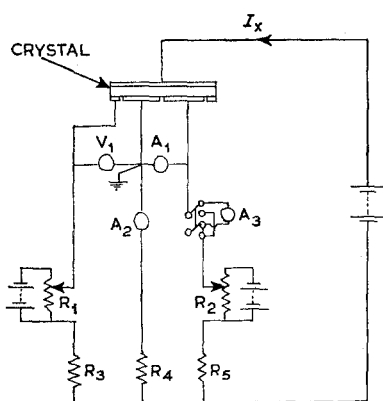


Figure 4 Circuit for Hall current measurement.

conditions (especially applied field strength), may be significant factors determining the conduction mechanism.

Provided single crystals of suitable size can be prepared the Hall current technique provides a powerful method of investigating the electronic properties of high resistivity single crystals. It may also prove of value in checking the microwave Hall mobility measurements made on polycrystalline protein samples [8, 9].

Acknowledgement

We wish to thank Mr G. Race for constructing the Hall current cell and assisting in its design.

References

1. V. N. DOBROVOLSKII and YU. I. GRITSENKO, *Soviet Phys. Solid State* **4** (1963) 2025.
2. R. PETHIG and K. MORGAN, *Nature* **214** (1967) 266.
3. K. MORGAN and R. PETHIG, *ibid* **223** (1969) 496.
4. A. SCHMILLEN and W. W. FALTER, *Z. Physik* **218** (1969) 401.
5. L. FRIEDMAN, *Phys. Rev.* **133** (1964) A1668.
6. M. SCHADT and D. F. WILLIAMS, *Phys. Stat. Sol.* **39** (1970) 223.
7. R. W. MUNN and W. SIEBRAND, *Chem. Phys. Letters* **3** (1969) 655.
8. E. M. TRUKHAN, *Pribory tekhn. eksper* **4** (1965) 198.
9. D. D. ELEY and R. PETHIG, *Bioenergetics* **1** (1970) 105.

Received 1 November
and accepted 7 December 1970

K. MORGAN
*Department of Electrical Engineering,
University of Southampton, Southampton, UK*
R. PETHIG
*Department of Chemistry,
University of Nottingham, Nottingham, UK*

Note on X-ray line Broadening and Electron Microscopy Study of the Effects of Milling and Subsequent Annealing of Alumina Powders

Various workers have observed the effects of milling and explosive shock in ceramic powders by X-ray line broadening [1-4], but no investigations have correlated the results with electron microscopy in deformed oxide ceramic powders, and the effect of annealing. The present work describes the observations made by X-ray line broadening and electron microscopy on the effects of impact milling and subsequent annealing on high purity submicron alumina powders.

B.D.H. Analar grade α alumina of average 1 μm particle size and purity 99.988% was used for the present investigation.

5g charges of powder were impact milled for various times up to 48 h in an alumina cylinder with an alumina cretoid, using a Glen Creston vibratory mill.

X-ray powder profiles were obtained using a Philip's diffractometer with Ni filtered Cu K α radiation by step scanning at intervals of $1/8^\circ 2\theta$.

The profiles were analysed for crystallite size and strain by using the integral breadth method of Wagner and Aqua [5], the separation of α_2 component was obtained by Rachinger's method corrected for instrumental broadening by the parabolic relation.

The shape and size of the powder was examined in an EM6G electron microscope.

Milling produces broadening of the X-ray line profiles, which on analysis measured increase in strain and decrease in crystallite size of the

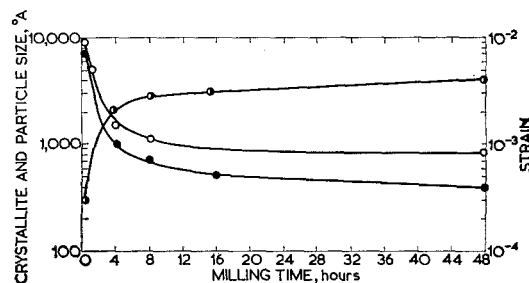


Figure 1 Variation of strain, crystalline size and particle size with milling. ● = strain. ● = crystallite size. ○ = particle size.